WPPMI-PR(18) 20923

M Siccinio et al.

On the figure of merit for the divertor protection in the preliminary design of tokamak fusion reactors

Preprint of Paper to be submitted for publication in
Nuclear Fusion

This work has been carried out within the framework of the EUROfusion Consortium and has received funding from the Euratom research and training programme 2014-2018 under grant agreement No 633053. The views and opinions expressed herein do not necessarily reflect those of the European Commission.

On the figure of merit for the divertor protection in the preliminary design of tokamak fusion reactors

M. Siccinio[1,2*], G. Federici[1], R. Kembleton[1,3], H. Lux[3], F. Maviglia[1,4], J. Morris[3]

[1] PPP&T Department, EUROfusion Consortium, Boltzmannstr. 2, 85748 Garching bei München, Germany
[2] Max-Planck-Institut für Plasma Physik, , Boltzmannstr. 2, 85748 Garching bei München, Germany
[3] EURATOM/CCFE Fusion Association, Culham Science Centre, Abingdon, Oxon, OX14 3DB, United Kingdom
[4] Consorzio CREATE, Università di Napoli Federico II, Naples, Italy

*Corresponding author. Tel.: +49 (0)89-3299-1843. E-mail address: mattia.siccinio@euro-fusion.org

Abstract

This paper discusses the criteria to be employed in the preliminary phases of a tokamak fusion reactor dimensioning to ensure the compatibility of the divertor heat load, without at the same time compromising the stability of core plasma or the fusion power generation. The analysis focusses on the inter-ELMs phase, and also neglects major off-normal events like disruptions. It is shown that two high-level requirements are necessary to be fulfilled, namely 1) the concentration of seeded impurities in the SOL has to be lower than some critical value in order not to compromise the fusion plasma performance or stability and 2) the damage of the divertor plate in case of accidental plasma re-attachment must be avoided for a time sufficiently long to ensure a safe, controlled termination of the plasma discharge. Two figures of merit, corresponding to such criteria, are identified in the existing literature and discussed. Also, the dependence of such figures of merit on the relevant machine design parameters is analysed, first by employing a simple, 0D physics approach and secondly by means of the systems code PROCESS [1,2], which allows the inclusion of further physics and technological constraints. The main conclusion of the present work is that, for a given fusion power level, the contemporary fulfilment of both requirements limits the viable reactor size both in terms of minimum major radius R and in terms of maximum toroidal magnetic field B.

1. Introduction

To achieve a satisfactory performance in terms of net electric power output, tokamak fusion reactors have to possess adequately large magnetic fields and size in terms of major radius R, in order to confine the burning plasma for a sufficiently long time. The European demonstrative reactor EU-DEMO [3], for example, possesses a major radius $R\sim$ 9 m and it is operated with a magnetic field on the axis B of around 6 T, and it is expected to yield a fusion power P_{fus} of around 2 GW if the confinement time τ_E obeys to the widely employed IPB98(y,2) scaling [4]. Note that the design of the EU-DEMO is at the moment in the so called pre-conceptual design analysis, thus the values of major radius and field are still subject to change. In this work, the indicative values 9 m and 6 T for R and B are henceforth assumed for a DEMO reference reactor, in order not to relate our work to any provisional design, but rather to remain on a general level. The relevant engineering parameters of such reference reactor are summarised in table 1.

Quantity	Values	Unit
R	9	m
B	6	T
q_{95}	3.5	
A	3.1	
f_{LH}	1.2	
P_{fus}	2000	MW
P_{LH}	110	MW
$\frac{P_{sep}B}{q_{95}AR}$	7.7	MW T m^{-1}
$\hat{c}_{Z,det}$	0.84	

Table 1. Relevant parameters of the chosen DEMO reference. The definition of the various quantities is to be found in the main text. Also, the value of $P_{sep}B/q_{95}AR$ and $\hat{c}_{Z,det}$ will be extensively discussed in section 2.2 and 2.3, respectively.

The reference plasma scenario for ITER and the EU-DEMO is the so-called.ELMy-H mode [5], which is known to exhibit a lower threshold on the charged particle power crossing the last closed magnetic surface P_{sep}, below which

the confinement capability of the machine is significantly reduced as the L-mode is recovered. Different empirical scaling for the threshold power P_{LH} exist, the most commonly utilised being the Martin scaling [6],

$$P_{LH} = 0.049 n^{0.72} B^{0.8} s^{0.94} \quad (1)$$

which will be employed in the following of the present work – here, n is the (line averaged) plasma density expressed in 10^{20} m^{-3} units, and s is the plasma surface, whereas P_{LH} is expressed in MW. All available scaling, however, clearly point out that such threshold power P_{LH} increases both with the magnetic field and with the size of the device. The same argument applies, at least qualitatively, also to other possible plasma configurations alternative to the ELMy H-mode, as for example the QH-mode [7] and the I-mode [8] - although these regimes are at the moment less investigated than the ELMy-H mode, and no well-established, quantitative scaling laws for the transition power are available yet.

For this reason, it is legitimate to expect the problem of the divertor compatibility to become more severe when the "size" of the reactor (here intended both in terms of radius and of magnetic field) increases, independently on the chosen plasma configuration. Most of the reactor designs currently investigated are assumed to operate with an at least partially detached divertor, implying that a significant fraction of P_{sep} will be dissipated in the scrape-off layer (henceforth SOL) before actually reaching the target plate. This reflects the fact that the power striking on the plates would otherwise be too high to be dealt with by current state-of-the-art of high heat flux technology. The necessary high dissipation is planned to be obtained with the use of seeded, radiative impurities, such like Ar or Kr [9], which re-distribute the necessary fraction of the exhaust power onto the first wall in form of photons. The employment of these impurities is however not without consequences for the machine operation. A certain fraction of the seeded atoms, in fact, is expected to migrate into the plasma core, where, depending on the edge profile characteristics, can cause either a reduction of the fusion power via fuel dilution or trigger some radiative instability [10]. It is therefore necessary to find an adequate balance between the radiation level in the SOL and the impurity content in the core, but it is not a-priori obvious whether this is feasible for every machine configuration. Additionally, it has to be considered that the radiated power is not "lost" but spread around nearby surfaces, and must be accounted for in the design of the plasma-facing components.

Furthermore, divertor detachment is a condition that can be lost, for example as a consequence of a failure of the impurity seeding system, or after a large fluctuation in the separatrix power (e.g. an unmitigated ELM) , or also for a density fluctuation in the divertor region. For machines like DEMO and ITER, where a large amount of nuclear reactions are taking place and whose construction is therefore subject to a nuclear licencing procedure, it is essential to demonstrate that a strategy to safely terminate the plasma discharge without compromising the integrity of the machine in case of incidental re-attachment is available. Clearly, this strategy depends on how large the flux on the target plate in case of divertor re-attachment is, which also determines the time available to restore detachment, or to terminate the discharge. One of the points discussed in this work is actually that the necessity of such a strategy implies the existence of an upper limit on the tolerable power load at the target plates by re-attachment.

In this analysis, both the role of the edge localised modes (ELMs - which are the main feature of the ELMy-H mode and are well-known to be a very severe issue when extrapolated to a reactor scale [11], and for which no obvious power-plant relevant solution seems to be available), and major off-normal events such like disruptions, are neglected. Instead, the analysis is concentrated on the discussion about the necessary criteria which have to be considered in the preliminary design phase for a tokamak fusion reactor to ensure divertor protection, which is acknowledged to be one of the most problematic aspects in view of the realisation of fusion power plants. This investigation is intended to provide a conceptual framework for the early phases of tokamak dimensioning, and does not purport to enter in the physics and engineering detail of the divertor design.

The paper is structured as follows: in section 2, the criteria which have to be considered for the divertor protection are discussed, and suitable figures of merit to compare different reactor configurations on the basis of such criteria are identified in the published literature. In section 3, the dependence of such figures of merit on the relevant design parameters, namely R and B, is analysed, first by employing a simple, 0D physics argument and secondly by means of the systems code PROCESS [1,2], which allows the inclusion of further technological constraints. Conclusions are drawn in section 4.

2. Criteria and figures of merit for the divertor protection

As discussed in the introduction, in order to ensure a safe operation for the divertor of a fusion reactor, the two following conditions are necessary to be fulfilled:

1) The machine must be able to survive in case of divertor re-attachment for a time interval which is sufficiently long to allow a safe, controlled termination of the plasma discharge, or a recovery of

detachment. The re-attachment of the divertor is an unlikely event, which however cannot be excluded, also by virtue of the somehow limited available diagnostics which are expected to be compatible with the operation in a high neutron fluence environment like an electricity producing reactor. A strategy to ensure the integrity of the target plate in case of loss of detachment is therefore a necessary requirement, which has to be taken into account since the very preliminary design phases, as these requirements can drive machine dimensioning and hence impact on other systems. The strategy itself depends on how high the heat flux on the target plate will be in case of a loss of detachment. Thus, this criterion naturally translates into a limit on the maximum tolerable power crossing the separatrix divided by the magnitude of the wetted area when detachment is lost.

2) The divertor detachment must be achievable with an impurity content in the SOL which is sufficiently low to avoid the risk of radiative instabilities in the plasma edge – possibly leading to major plasma disruptions - and/or to excessively deteriorate the fusion power yield as a consequence of fuel dilution [10].

In the following, those criteria will be expressed in terms of quantitative figures of merit taken from the existing literature, which will allow a direct comparison of different reactor configurations.

2.1. Figure of merit – heat flux by re-attachment

All future fusion power plants will have to be shown to be able to safely terminate, or recover, the plasma discharge without compromising the machine integrity in case of off-normal events. For the divertor, this means essentially being able to withstand the heat flux by re-attachment without attaining coolant burn-out conditions for a sufficiently long time in case a loss of detachment – no matter the cause - occurs. The ability of surviving a re-attachment event depends on the magnitude of the heat flux q_{tar} which strikes on the divertor by a detachment loss, which can be written as

$$q_{tar} = \frac{P_{sep}}{2\pi\lambda_{int}R}\, f_{geo} \tag{2}$$

where λ_{int} is the power decay length for the heat load at the divertor plate and $f_{geo} = \sin(\eta)$ is a factor that takes into account the inclination of the divertor plate with respect to the magnetic field line (the angle η is the angle between the striking magnetic field line and the divertor plate in the poloidal plane).

The decay length on the target plate λ_{int} is related to the decay length at the outer midplane λ_q via the relation

$$\lambda_{int} = \lambda_q + 1.64S \tag{3}$$

It is expected that the parameter S, which mimics the broadening of the heat channel in the divertor volume by effect of perpendicular transport processes, is more effective in large devices like DEMO than in the existing machine, mainly by virtue of a larger divertor volume (incidentally, the role of poloidal and toroidal flux expansion is conservatively not considered, as it is supposed not to be too relevant in the DEMO lower single null divertor configuration). We assume for this reason

$$S = 2\lambda_q \tag{4}$$

The power decay length λ_q, which is proportional to λ_{int} according to Eq.2 and 3, scales as suggested by the Eich scaling [12,13],

$$\lambda_q = 0.73B^{-0.78}q_{95}^{1.2}R^{0.1} \tag{5}$$

where q_{95} is the value of the safety factor on the magnetic surface which encloses the 95% of the magnetic flux of the confined plasma. Eq.5 is approximated by

$$\lambda_q \propto \frac{1}{B_p} \tag{6}$$

where B_p is the poloidal magnetic field strength. Thus, in view of Eq.2 and 6, the heat flux by re-attachment can be estimated by

$$q_{tar} \propto \frac{P_{sep}B_p}{R} \sim \frac{P_{sep}B}{q_{95}AR} \tag{7}$$

where A is the aspect ratio. The figure of merit which will be employed to ensure that the heat load by re-attachment is tolerable can therefore be expressed as

$$\frac{P_{sep}B}{q_{95}AR} < \left.\frac{P_{sep}B}{q_{95}AR}\right|_{REF} \tag{8}$$

as already suggested in ref. [14]. The value of $P_{sep}B/q_{95}AR\big|_{REF}$ is discussed in detail in the next subsection.

2.2. Heat Load by Re-attachment and Divertor Sweeping

To calculate the heat load on the target plate in a machine like EU-DEMO when the divertor is attached, the same, simplified approach elucidated in [15] is adopted. First, one has to determine the wetted area A_W on which the heat is deposited, following Eq.2, as

$$A_w = \frac{2\pi R \lambda_{int}}{f_{geo}} \tag{9}$$

Assuming that only 2/3 of the power crossing the separatrix lands on the outer target, and that a $f_{loss} = 20\%$ fraction of the entering power is dissipated in the SOL by various processes (e.g. charge exchange, hydrogen radiation, residual impurity radiation) even in absence of detachment, the value of the heat load on the divertor plate by re-attachment q_{tar} is found to amount to

$$q_{tar} = \frac{2}{3}(1 - f_{loss})\frac{P_{sep}}{A_w} \tag{10}$$

The actual DEMO divertor is able to tolerate heat fluxes up to ~15-20 MW m^{-2} [16]. However, simulations performed with the code RACLETTE [17] and shown in Fig. 1 indicate that, in presence of an heat load of about 40 MW m^{-2} (i.e. twice as large) the employment of the divertor sweeping [18,19] can allow the target surviving for a time which is compatible with typical actuator delays (tens of seconds). On the contrary, if no active control is employed (ss – red curves), burn-out in the coolant is reached in less than two seconds (other criteria, as for example the temperature of the W layer and of the CuCrZr pipe, have been found by RACLETTE to be less critical, and are therefore not shown). In other words, without sweeping, the timescales of the occurring damages are too short for the implementation of a robust strategy which allows the controller to safely terminate the plasma discharge without compromising the integrity of the machine components.

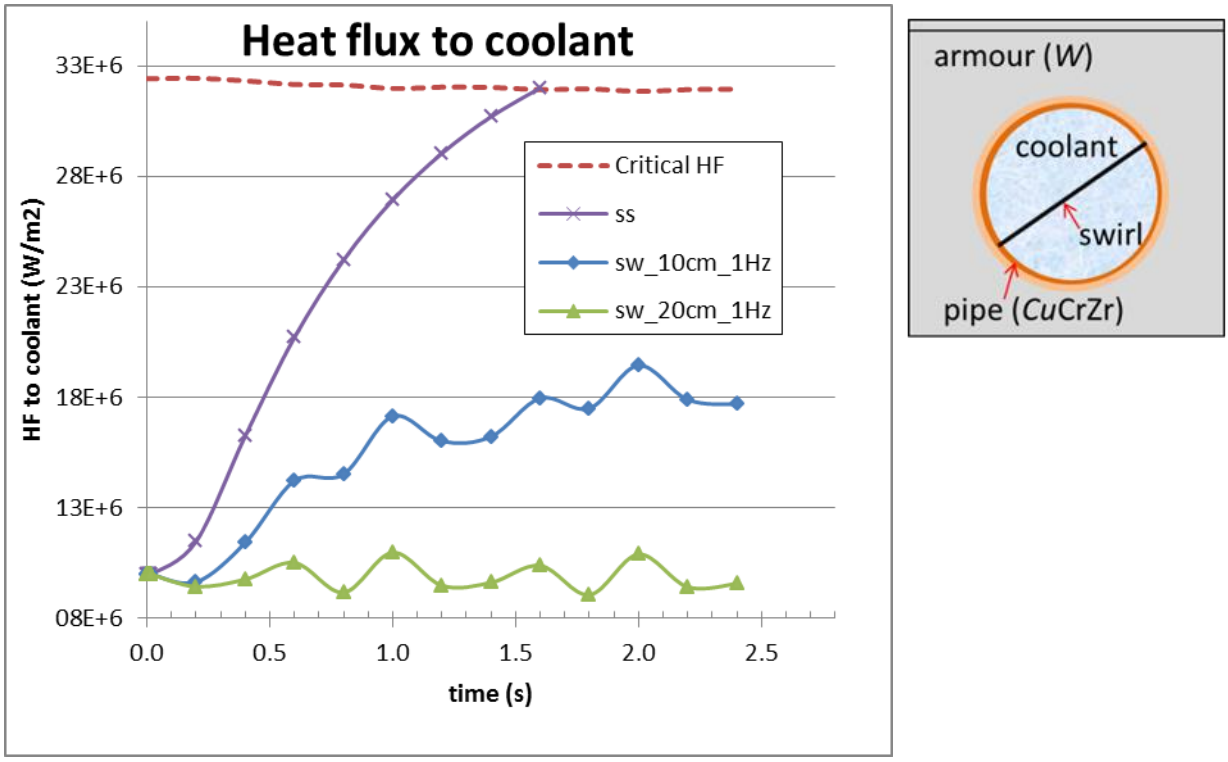

Figure 1. Temperature and heat load transients in the divertor armour and cooling pipe when exposed to a heat flux q_{tar}= 40 MW/m^2, starting from a foreseen flattop value of 10MW/m^2. The structure of the divertor element is shown in the lower right corner of the figure, with the W layer being exposed to the plasma chamber. The figure on the left shows the evolution of the heat flux reaching the coolant, with the black dashed line indicating the critical heat flux. Blue and green lines indicate behaviour under different divertor sweeping amplitudes (see main text). These figures have been produced with calculations of the code RACLETTE.

During the divertor sweeping the position of the strike points on the divertor plate is moved periodically in the poloidal direction with a certain amplitude and frequency. This allows spreading the power on a larger surface than in absence of sweeping.

The effect of the divertor sweeping can be shown to be extremely beneficial. Back to Fig.1, one can observe that with a sweeping frequency of 1 Hz and a spatial extent of ±10 cm around the unperturbed strike point (blue curves), the critical heat flux is never reached. The calculation for the case by 1 Hz and of ±20 cm (green curves) is even more beneficial, bringing the heat flux to values comparable to the detached case – and also, the tungsten remain below the recrystallization temperature and the CuCrZr pipe does not reach the softening temperature, more details on this to be found in [18,19].

The possibility of employing the divertor sweeping in DEMO is at this stage still speculative, as there are many open points to be addressed, both on the physics side (e.g. is the divertor sweeping compatible with the stability of the plasma discharge during a fast, controlled termination?) and on the engineering. Also, from an operative point of view, it is crucial to define a criterion for the diagnostics to ensure the sweeping to be already active when the plasma re-attaches, or shortly after – for reasons linked to fatigue effects, it is not possible to maintain the sweeping during standard operation, it has to be understood as an emergency procedure, a detailed analysis on this can be found in [18,19]. These questions, however, are far beyond the purposes of the present manuscript. For the time being, it is assumed that *it is possible for a machine with divertor sweeping to tolerate an heat flux equal to, but not larger than, 40 MW/m2 for a sufficiently long time to allow a controlled termination of the discharge*.

By employing the Eich scaling Eq.5, as well as Eq.3 and 4, and using the DEMO reference parameters in table 1, the width of the power channel at the outer midplane can be evaluated, finding $\lambda_q = 1.34$ mm and $\lambda_{int} = 5.73$ mm. Assuming $\eta = 30^o$, one finds then A_w= 1.94 m^2. An heat flux $q_{tar} = 40$ MW m^{-2}, in view of Eq. 10, corresponds to a power at the separatrix $P_{sep} \approx 150$ MW. In terms of the figure of merit $P_{sep}B/q_{95}AR$, Eq.8 translates into

$$\frac{P_{sep}B}{q_{95}AR} < \sim 9\ MW\frac{T}{m} \tag{11}$$

This reference value will be used in the following of the present work as a limit value. For the reference DEMO, this value would correspond to $f_{LH} \approx 1.4$. Correspondingly, at f_{LH}= 1.2, one finds $P_{sep}B/q_{95}AR$ = 7.7 MW T m^{-1}, as reported in table 1.

2.3. Figure of merit – critical impurity concentration

As previously discussed, it is expected that a future fusion power plant will be run, as ITER, with a (partially or fully) detached divertor, such detached condition being achieved, and maintained, via injection in the SOL of seeded radiating impurities. However, the content of impurities in the SOL cannot be arbitrarily high, as, if their concentration in the confined plasma region (in turn expected to be linked to the concentration in the SOL via some compression factor c_F) exceeds some critical value, the plasma performance will be compromised, either in terms of stability because of an excessive radiation in the pedestal, or via fuel dilution. The link between the impurity concentration in the scrape-off layer and in the core plasma is not straightforward to be determined, as it depends on impurity transport mechanisms whose extrapolation to reactor relevant scales is not completely clear. In current experiments, a compression factor c_F

$$c_F = \frac{c_{Z,SOL}}{c_{z,core}} \tag{12}$$

of the order of ~5 is observable [20], with different behaviour for different impurity species [21] (here, c_Z identifies the concentration of the generic impurity Z).

In a recent publication by Reinke [22], a simple 0D argument has been suggested to estimate the necessary concentration of impurities $c_{Z,det}$ to obtain divertor detachment for a given tokamak machine, with known engineering parameters. Neglecting some factors which will be kept constant in our analysis, the Reinke formula (Eq.10 in [14]) reads

$$c_{Z,det} \propto \frac{f_{LH}^{1.14}B^{0.88}R^{1.33}q_{95}^{0.39}}{A^{0.59}} \tag{13}$$

where f_{LH} is the ratio between P_{sep} and P_{LH}, the latter evaluated by means of the Martin scaling [6]. Note that such formula could, at least in a first approximation, be adapted also for reactors conceived for QH-mode or I-mode

operation, simply understanding f_{LH} as a ratio between the power at the separatrix and the corresponding Martin scaling value, even if the threshold power for this regimes does not follow the Martin scaling. However, the Reinke formula is based on the Eich scaling [12,13] for the power decay length in the SOL λ_q, and it is unclear whether such scaling can be applied to QH-mode and I-mode as well – it is known that it has almost the same dependence on plasma parameters both in H-mode and in L-mode. Although the Reinke scaling is probably oversimplified to be employed for a quantitative evaluation of the necessary impurity concentration, it provides nevertheless a useful criterion to express how such concentration varies in dependence of some relevant machine parameters, thus representing a useful tool for comparing different machines and/or configurations. The figure of merit for the critical impurity concentration can then be expressed as

$$c_{Z,det} < c_{Z,REF} \tag{14}$$

where $c_{Z,REF}$ is a certain reference value, which has to be chosen to guarantee the machine operation with some margin. A machine like the reference DEMO is still, although marginally, operable with the required impurity concentration to detach the divertor [23]. In this paper, with some degree of arbitrariness, it is assumed $c_{Z,REF}$ to be equal to the DEMO value of $c_{Z,det}$ if P_{sep} =150 MW – which corresponds to $f_{LH} \approx 1.4$, as already stated in the previous subsection. In other words, *we assume that at* f_{LH} = 1.4, *the reference DEMO would be operated at the maximum tolerable value for both figures of merit at the same time*. Eq.14 can therefore be recast as

$$\hat{c}_{Z,det} < 1 \tag{15}$$

where the $\hat{}$ indicates quantities normalised to the mentioned reference DEMO at $f_{LH} \approx 1.4$. Strictly speaking, if a reactor configuration is operated at $\hat{c}_{Z,det} > 1$, it possesses an impurity concentration in the SOL (and thus in the core, assuming identical compression factors) larger than what the reference DEMO would require to maintain the detachment at 150 MW. In reality, this occurrence is not necessarily implying that the stability of the scenario or its fusion yield are compromised – more careful analysis would be required at that point. However, it is reasonable to assume that the reference DEMO at f_{LH} = 1.2 operates close to the maximum tolerable impurity concentration, but still has some margin, this choice been at least approximatively justified by the simulations presented in ref. [10]. In view of Eq.13, the reference DEMO at f_{LH} = 1.2 possesses $\hat{c}_{Z,det}$= 0.84, as stated in table 1.

3. Feasible points in the $R - f_{LH}$ plane

The goal of the following calculations is to express the two relevant figures of merit for the divertor protection elucidated above – namely $P_{sep}B/q_{95}AR$, which estimates the heat load on the target plates by attached conditions, and $\hat{c}_{Z,det}$ (Reinke criterion), which considers the possibility of detaching the divertor without compromising the core plasma - as a function of f_{LH}, of the major radius R and of the aspect ratio A. The analysis will be carried out with the purpose of identifying the reactor configurations which are most favourable in terms of divertor protection.

In this analysis, the following quantities have been kept constant:

- **Fusion power P_{fus}**,
- **Edge Safety factor q_{95}** (it is assumed that the value of q_{95} is always chosen to be the minimum which allows a sufficient stability margin against disruptive events)
- **Greenwald fraction f_{GW}** (the machine is supposed to be operated at the maximum density value compatible with the density limits)
- Other shape factors (elongation, triangularity, etc…), as their role is not considered in the present analysis.

At first, the design space where the constraints on the two previously discussed figures of merit are fulfilled is identified by means of a simple 0D argument. Subsequently, results of the systems code PROCESS, which allow taking into account also other technological and physical limitations, are shown.

3.1. 0D Model

As by definition $P_{sep} = f_{LH}P_{LH}$, the previously mentioned Martin scaling [6] is employed for P_{LH},

$$P_{LH} \sim n^{0.72}B^{0.8}s^{0.94} \tag{16}$$

(here and in the following, constant factors are not written). We can assume the surface s to be proportional to $aR \sim R^2/A$, where a is the minor radius. In turn, the plasma density n is linked to the plasma current I_p via the Greenwald fraction $f_{GW} = \pi n a^2/I_p$, which has been assumed to be constant,

$$n \propto \frac{I_p}{a^2} \tag{17}$$

The plasma current I_p can be written as a function of R, B and A by exploiting the constancy of q_{95} and of the shape factors

$$I_p \sim \frac{a^2 B}{R q_{95}} \sim \frac{RB}{A^2} \tag{18}$$

This implies

$$n \sim \frac{I_p}{a^2} \sim \frac{B}{R} \tag{19}$$

The LH threshold power P_{LH} in Eq.16 can be expressed as a function of R, B and A in the following way

$$P_{LH} \sim n^{0.72} B^{0.8} \frac{R^{1.88}}{A^{0.94}} \sim \frac{B^{1.52} R^{1.16}}{A^{0.94}} \tag{20}$$

In order to eliminate the B dependence, the constancy of the fusion power is exploited. Neglecting other constant factors, the fusion power P_{fus} scales as [24]

$$P_{fus} \sim \beta_N^2 \frac{B^4 R^3}{A^4} \sim p^2 \left(\frac{RB}{A I_p}\right)^2 R^3 \sim p^2 \frac{R^3}{A^2} \tag{21}$$

having enforced the dependence of I_p on R, B and A derived in Eq.18. The average pressure p, which enters via the normalised pressure parameter β_N,can be understood as the value of the (diamagnetic) energy W per unit volume V, where

$$V \sim \frac{R^3}{A^2} \tag{22}$$

In turn, the energy W can be thought of to be proportional to P_{fus} (constant) times the confinement time τ_E (note that these assumptions imply neglecting any auxiliary power source, i.e. it is assumed that the machine is ignited or at least with a sufficiently high gain Q).

$$P_{fus} \sim \frac{\tau_E^2}{R^6} A^4 \frac{R^3}{A^2} \sim \frac{\tau_E^2}{R^3} A^2 \tag{23}$$

Neglecting the influence of the core radiation on the confinement, the standard, non-radiation corrected IPB98(y,2) scaling [4] is employed,

$$\tau_E \sim I_p^{0.93} B^{0.15} n^{0.41} R^{1.97} A^{-0.58} P_{loss}^{-0.69} \tag{24}$$

The power entering the scaling law, P_{loss},is assumed to be equal to the α-particles heating power P_α, which is proportional to P_{fus}, thus constant in the present calculation and therefore not considered in the following. The assumption $P_{fus} \propto P_{loss}$ is consistent with the employment of IPB98(y,2), where the role of core radiation in determining the confinement time is not considered. In PROCESS, the power radiating from the innermost region of the plasma core (i.e. ρ_T < 0.6, according to [25,26], where ρ_T is the normalised toroidal flux coordinate) is subtracted from the loss power in the confinement time scaling law as it is assumed not to play a role in the conducted power losses driving the processes captured by the scaling law. This leads to some differences of behaviour between the approach here and the PROCESS results in Fig.4 below. The influence of the core radiation on the confinement time is still unclear and to some extent debated in the transport community; however for typical DEMO parameters, where the core (ρ_T < 0.6) radiation is ~25% of P_α, the difference between the two approaches is normally around 10-15%.

In view of the equations 18, 19 and 24, the scaling for the confinement time can be recast as

$$\tau_E \sim \left(\frac{RB}{A^2}\right)^{0.93} B^{0.15} \left(\frac{B}{R}\right)^{0.41} R^{1.97} A^{-0.58} \sim R^{2.49} B^{1.49} A^{-2.44} \tag{25}$$

Eq.25 can thus be employed to express B in terms of R and A, first by writing

$$P_{fus} \sim \frac{\tau_E^2}{R^3} A^2 \sim R^{1.98} B^{2.98} A^{-2.88} \tag{26}$$

Then, as the fusion power has been assumed constant, one can conclude

$$B \sim R^{-0.66} A^{0.97} \tag{27}$$

The LH threshold power P_{LH} can be now re-written by substituting B in Eq. 20 with the value in Eq. 27, obtaining

$$P_{LH} \sim \frac{B^{1.52} R^{1.16}}{A^{0.94}} \sim R^{0.16} A^{0.53} \tag{28}$$

With the help of Eq. 28, and recalling that $P_{sep} = f_{LH} P_{LH}$, the two figures of merit for the divertor protection can be expressed as a function of f_{LH}, A and R only

$$\frac{P_{sep} B}{q_{95} A R} \sim f_{LH} R^{-1.5} A^{0.47} \tag{29}$$

$$\hat{c}_{Z,det} \sim f_{LH}^{1.14} R^{0.75} A^{0.26} \tag{30}$$

Focusing for the moment on a constant value for the aspect ratio, it is convenient to represent the two figures of merit on a $f_{LH} - R$ plane. The magnetic field, as a consequence of Eq.27, varies as a function of the major radius only. In Fig. 2, the chosen reference DEMO (f_{LH} = 1.2) is depicted as a red point, and the curves at constant $\hat{c}_{z,det} = 1$ and $P_{sep} B / q_{95} A R = 9$ MW T/m are represented. Also, a lower limit on f_{LH} has been imposed, as a reactor has to be operated above the LH threshold in order to avoid H-L back transition, which might cause severe control issues and potentially lead to a disruption (as the favourable effect of the high-Z impurities on P_{LH} has been neglected, it is assumed that $f_{LH} \approx 1$ is still an acceptable work point).

The most relevant fact to be observed in Fig.2, which is a direct consequence of Eq.29 and 30, is that the critical impurity concentration $\hat{c}_{Z,det}$ scales favourably with the magnetic field and unfavourably with the radius, whereas $P_{sep} B / q_{95} A R$ scales favourably with the radius and unfavourably with the field. In other words, for a given fusion power level, *there will always exist an upper limit to the major radius above which the impurity concentration will be intolerably high, but also a lower limit to the major radius below which no technology is available to deal with the heat load on the target in case of re-attachment.*

In Fig.2, the region of the parameter space where the reactor operation would be more convenient with respect to the DEMO reference in terms of both figure of merits is shaded in green, and marked with the letter B. As one can see, most of the points in that region foresee an operation with a power at the separatrix closer to P_{LH} than what currently planned for DEMO – possibly exacerbating the problem of H-mode controllability, although with potentially more margin on the impurity concentration control. On the contrary, points in the regions A, D, E and F are not suitable for a reactor operation. More in detail

1. Points in A operate below the L-H threshold, thus are not providing the required fusion power in view of the insufficient confinement
2. Points in E are; unsuitable with respect of both figures of merit
3. Points in D are unsuitable with respect to the Reinke criterion, thus requiring an excessively high impurity concentration to maintain detachment
4. Points in F are unsuitable in terms of $P_{sep} B / q_{95} A R$, thus unable to deal with loss of detachment with the current heat removal technology

The meaning of the red shaped area marked with the letter C is discussed more in detail in the next sub-section.

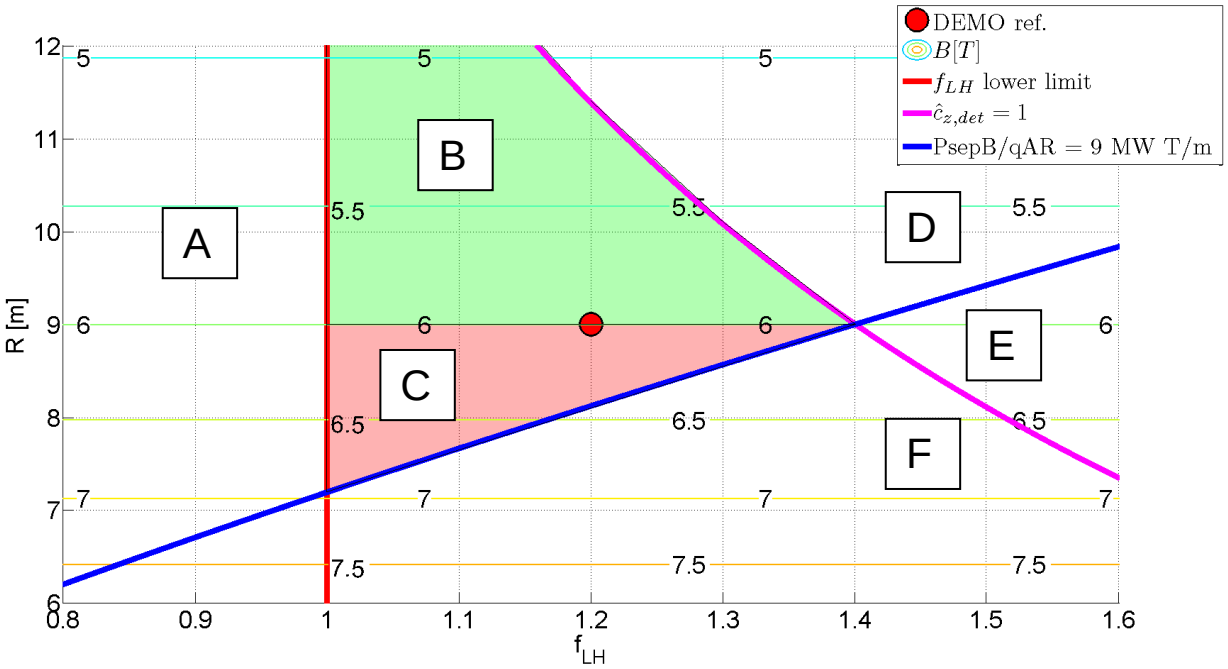

Figure 2. Representation of the constant $\hat{c}_{z,det} = 1$ and $P_{sep}B/q_{95}AR = 9$ MW T/m in the $f_{LH} - R$ plane, the fusion power being assumed as constant. The design point DEMO reference is denoted with a red point. The red vertical line identifies a lower limit of f_{LH}, under which the reactor operation is not feasible for the high risk of H-L transition. The green shaded area identifies the region of the parameter space which is more favourable than the reference DEMO with respect to both figures of merit. The red shaded area which is more favourable than EU-DEMO but necessitates an improved magnetic field coil technology to allow larger fields in a smaller machine. A more detailed description of regions A-F is to be found in the main text.

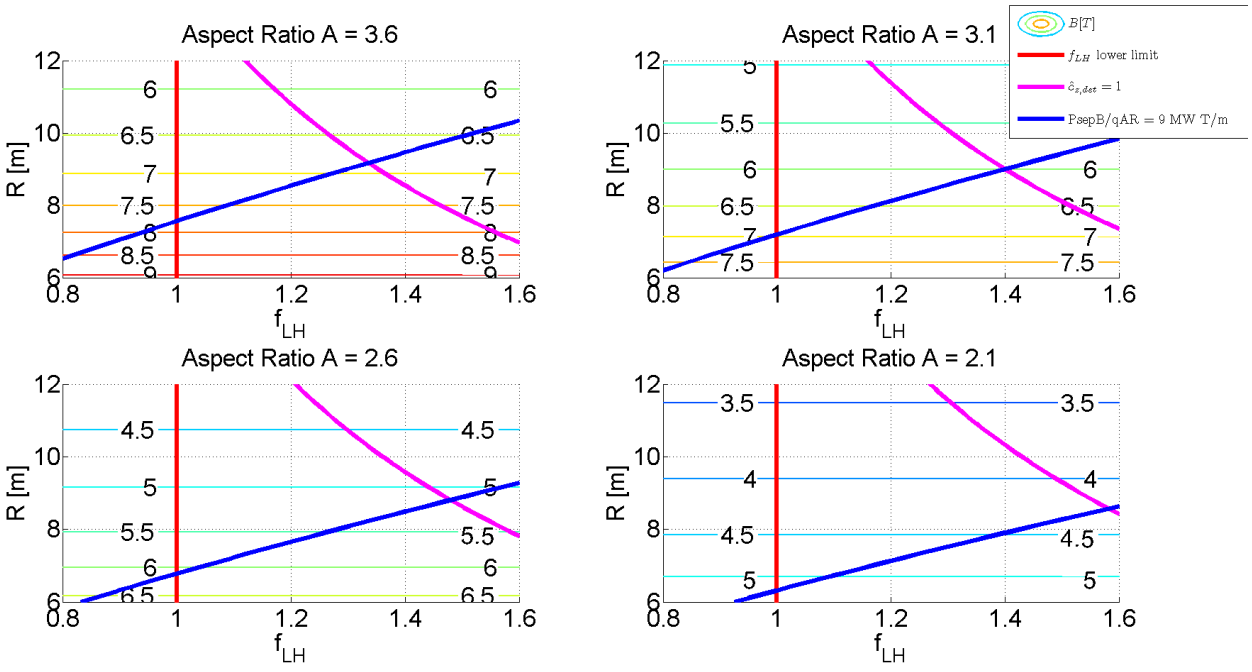

Figure 3. Same as Fig.2 for different aspect ratios. Lowering the aspect ratio has a beneficial effect on the divertor protection problem, allowing operation at higher f_{LH}. The fusion power is kept constant, thus the magnetic field decreases, at the same radii, by lowering the aspect ratio – as the plasma volume increases.

It is incidentally interesting to note that, according to Eq.29 and 30, the reduction of the aspect ratio is beneficial for both figures, as it increases the region of feasible operational points in terms of R and f_{LH}. This can be visualised in Fig.3.

3.2. Improved magnet technologies and power increase

In the previous sub-section, it has been shown that, given a certain fusion power lever, there exists both an upper and a lower limit for the tokamak major radius, beyond which at least one of the two criteria for the divertor

protection is violated. However, that conclusion was based only on physical arguments. In reality, once the technological constraints are enforced, one can demonstrate that it is not possible to reach an arbitrarily high magnetic field on a machine of arbitrarily low size. This is due to the fact that high magnetic fields are indissolubly linked to higher stress on the TF coils themselves, whose structure has then to be reinforced and made thicker, thus reducing the available space for the plasma and ultimately preventing the major radius to be decreased. This is exacerbated by the need for there to be a substantial thickness of material between the plasma and the TF coil for shielding (and probably tritium breeding) which is size-independent, meaning that the coil is proportionately further from the plasma in smaller machines. The current EU-DEMO design foresees that the TF coil thickness is such, that the structural material operates close to its stress limit (660 MPa for steel), which is equivalent to say that any increase in the field at the coil will automatically cause an increase in the major radius as well in view of the necessity of reinforcing the coil.

In the red shaded region of Fig.2, marked with the letter C, points which are better than the current DEMO design in terms of both divertor figures of merit, but who are not compatible with the technological radial build constraints just discussed, are shown. In order to access that region, a different TF coil design, able to produce higher fields with a smaller size, would be required. Further gains may also be made if the requirements on the central solenoid can be reduced and it can also be made smaller.

The interesting fact to be observed, however, is that *even if a technology able to produce arbitrarily high fields at reduced dimension would exist, the benefit on the machine design will be extremely limited*, as in the best case one could obtain a ~1.5 m reduction in the major radius at the price of operating the machine at lower f_{LH} (see Fig.2). In fact, higher fields are unsustainable because they cause the heat flux by re-attachment to rapidly increases to intolerable values.

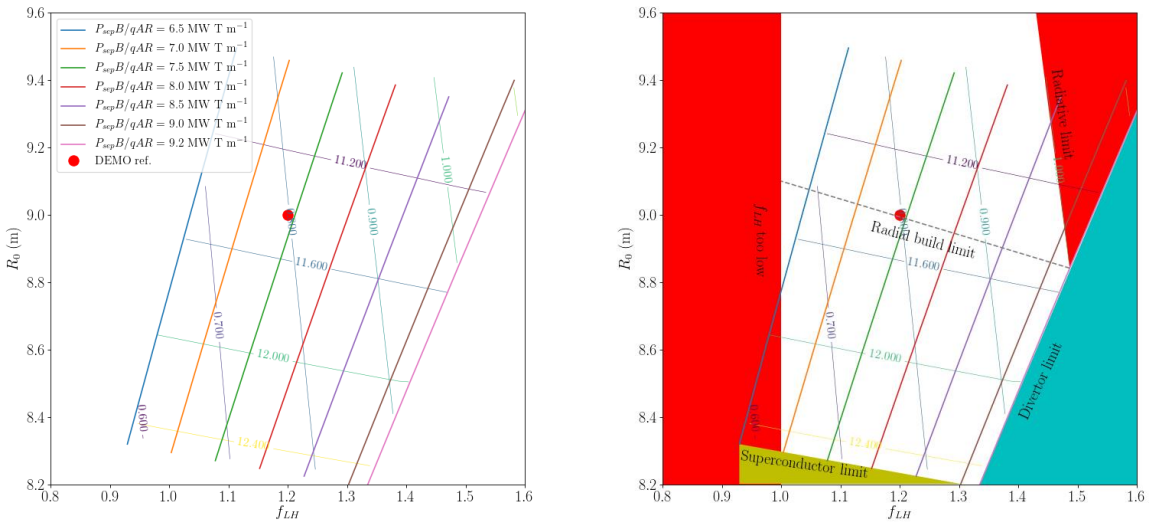

Figure 4. A mapping of the parameter space plotted using the PROCESS systems code employing more comprehensive interactions between the performance limiting factors. The constant $P_{sep}B/q_{95}\,AR$ curves are intersected by curves at constant B_{peak} (almost horizontal) and at constant $\hat{c}_{z,det}$ (pointing downwards), with the corresponding value written on the line. The reference DEMO is again denoted by a red dot. In the figure on the right, the points of the parameter space which are unsuitable for a reactor operation are shaded with different colours. Note that the R interval on the y-axis is more restricted than in Fig.2.

This conclusion has been reinforced by simulations carried out with the system codes PROCESS, shown in Fig.4, which confirms what plotted in Fig.3.In particular, an investigation of the effect of varying the peak field B_{peak} on the toroidal field coil, which is much more relevant in terms of technology than the field B in the plasma was carried out. The fact that the curves at constant B_{peak} exhibit a slight dependence on f_{LH} is due to the fact that PROCESS makes a global optimisation of the machine. Thus, at fixed radius, if f_{LH}, increases, then the core radiation via impurity seeding decreases correspondingly. This allows PROCESS to reduce the size of the central solenoid in view of the lower Z_{eff}, so, at constant radius, there is more space for the TF coil and B_{peak} increases. In spite of the much more detailed description of the power plant available in PROCESS, the correspondence with the simple 0D argument reported in Fig.2 is pretty satisfactory (note that the R interval on the y-axis in Fig.4 is much more restricted than in Fig.2). This is a clear indication of the fact that *the divertor protection is the most relevant criterion for the dimensioning of a tokamak reactor*.

3.3. Extrapolation to larger devices

The analysis performed in the previous paragraphs was carried out at constant fusion power, with the purpose of identifying the "ideal" operation point for a machine of the size of DEMO. It is however interesting to explore the extrapolation towards larger machines, whose fusion power production is larger than the 2 GW of the reference DEMO – and correspondingly, a larger net electric power is expected.

In order to produce a larger fusion power than DEMO, either the field or the radius, or both, must increase. Assumed that for the time being A and q_{95} are kept constant, the calculation from Eq.24 to 26 is repeated, this time by retaining the P_{loss} term (as the fusion power is not any longer considered constant). This leads to

$$P_{fus} \propto B^{2.98} R^{1.98} P_{loss}^{-1.38} \tag{31}$$

which implies

$$P_{fus} \propto B^{1.25} R^{0.83} \tag{32}$$

(where again it has been assumed that $P_{fus} \propto P_{loss}$, see section 3.1). If f_{LH} is kept constant as well, following Eq.13, the Reinke criterion exhibits the following dependence on R and B:

$$\hat{c}_{Z,det} \propto B^{0.88} R^{1.33} \tag{33}$$

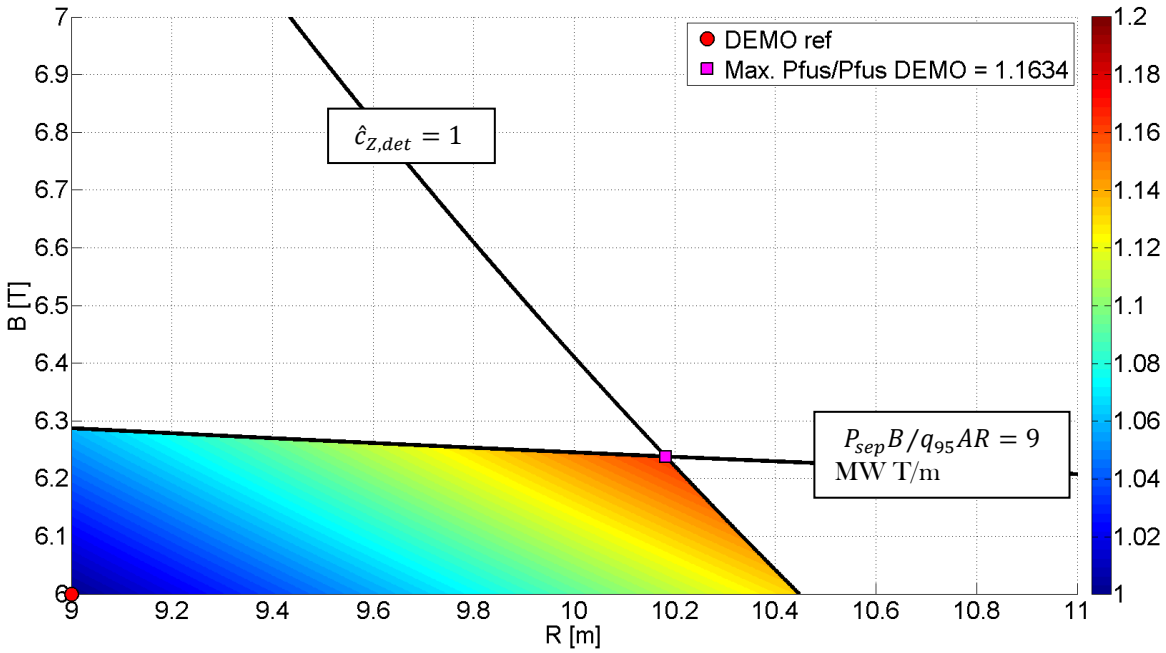

Figure 5. Fusion power level normalised to the reference DEMO value as a function of R and B. Points with $\hat{c}_{z,det} > 1$ and/or $P_{sep}B/q_{95}AR > 9$ MW T/m have not been displayed, as unfeasible. Also, the two limit curves are represented. Aspect ratio, q_{95}, f_{LH} and Greenwald fraction have been kept constant. The point corresponding to the reference DEMO is highlighted in red, whereas the feasible point with the maximum fusion power (i.e 1.16 timed the reference DEMO) is indicated with a magenta square.

Also, in view of Eq.20, it is straightforward to demonstrate that

$$\frac{P_{sep}B}{q_{95}AR} \propto B^{2.52} R^{0.16} \tag{34}$$

at constant Greenwald fraction. In Fig.5, in view of Eq.32, 33 and 34, the fusion power level corresponding to various R and B is displayed, excluding however all the points where at least one of the two figures of merit identified in the text above is not fulfilled. As one can observe, the fulfilment of the Reinke criterion has the effect of limiting the maximum size of the tokamak – as its dependence on the radius is stronger than the one on the field – whereas the $P_{sep}B/q_{95}AR$ limits on the contrary the magnetic field strength. As a result of the two figures of merit, the region of the parameter space where machines having a larger fusion power than DEMO possibly exist (at constant A, q_{95} and f_{LH}) is limited, and this also poses an upper limit to the maximum achievable fusion power –

1.16 times the reference DEMO value for the assumptions employed in the present analysis (with the caveat that other technical and eventually physical limitations not considered in this work might further reduce the number acceptable solutions).

Incidentally, if the power degradation in the confinement time scaling were ignored, the maximum achievable fusion power which can be obtained without violating the divertor constraints would rise up to ~1.43 in normalised units.

4. Conclusions

In this paper, the preliminary design criteria to ensure divertor protection in a tokamak fusion reactor have been discussed, and corresponding figures of merit to quantitatively compare different reactor configurations have been proposed. More in detail, the Reinke criterion has been employed to estimate the necessary concentration of seeded impurities to detach the divertor, while $P_{sep}B/q_{95}AR$ is utilised as a proxy for the heat flux on the divertor plate in case of plasma re-attachment. By means of a simple 0D argument it has been shown that, at constant fusion power, the two figures of merit possess opposite dependences on the major radius and on the magnetic field, and consequently there will always exist, for any given fusion power level, a maximum radius and a maximum magnetic field above which the divertor compatibility cannot be ensured, either because of a too high impurity concentration required to detach the divertor – which can compromise the stability or the fusion yield of the confined plasma – or because of a too high heat flux by re-attachment, which cannot be dealt with by the available heat flux technology. These constraints also pose a limit on the maximum fusion power achievable with a tokamak fusion reactor, as any increase in size and field will unavoidably worsen the divertor compatibility problem. The results obtained by the simplified 0D model have been confirmed by simulations carried out with the more detailed system code PROCESS, clearly pointing out that the divertor protection is the main size driver in the preliminary dimensioning of a fusion reactor. Also, one of the consequences of the present analysis is that an hypothetical magnets technology, able to provide very large fields at limited size, is not per se sufficient to impact significantly on the machine design, as the maximum allowable strength of the magnetic field, as previously stated, is essentially constrained by divertor protection considerations.

5. Acknowledgments

Enlightening discussions with P. Barabaschi, M. Wischmeier, A. Loarte, J. H. You and K. Lackner are gratefully acknowledged by the authors. This work has been carried out within the framework of the EUROfusion Consortium and has received funding from the Euratom research and training programme 2014-2018 under grant agreement No 633053. The views and opinions expressed herein do not necessarily reflect those of the European Commission.

6. References

1. Kovari M. et al., 2014 Fusion Eng. Des. **89** 3054
2. Kovari M. et al., 2016 Fusion Eng. Des. **104** 9
3. Federici G. et al., 2017 Int. Symp. on Fusion Nuclear technology (ISFNT), Kyoto, Japan
4. Uckan N.A. 1989 ITER physics design guidelines, ITERTN-PH-8-6
   (http://www.iaea.org/inis/collection/NCLCollectionStore/_Public/21/068/21068960.pdf?r=1)
5. Wagner F et al., 1982 Phys. Rev. Lett. **49** 1408
6. Martin Y.R. et al., 2008 J. Phys.: Conf. Ser. **123** 012033
7. Burrell K. H. et al., 2002 Plasma Phys. Control. Fusion **44**, A253
8. Ryter F. et al., 2017 Nucl. Fusion **57**, 016004
9. Wenninger R.et al., 2015 Nucl. Fusion **55** 063003
10. Siccinio M. et al., 2018 Nucl. Fusion **58** 016032
11. Zohm H. et al., 2013 Nucl. Fusion **53** 073019
12. Eich T. et al., 2011 Phys. Rev. Lett. **107** 215001
13. Eich T. et al., 2013 Nucl. Fus*ion* **53** 093031
14. Zohm H. *et al* 2017 *Nucl. Fusion* **57** 086002
15. Pitts R., York University Seminar 05.11.2015
    (https://www.york.ac.uk/media/physics/ypi/docs/Richard%20Pitts%20Seminar%20051115.pdf)
16. You J.H. et al., 2016 Nuclear Materials and Energy **9** 171
17. Raffray A.R.and Federici G., 1997 J. Nucl. Mater. **244** 85
18. M. Li et al., et al., 2016 Fusion Eng. Des. **109** 1067
19. Maviglia F. et al., 2016 Fusion Eng. Des. **109** 1067
20. Kallenbach A. et al., 2013 Plasma Phys. Control. Fusion **55** 124041
21. Bernert M. et al., 2017 Nuclear Materials and Energy **12** 111

22. Reinke M.L. 2017 Nucl. Fusion **57** 034004
23. Subba F. et al., 2018 Plasma Phys. Control. Fusion **60** 035013
24. Zohm H., 2010 Fusion Science and Technology **58:2** 613
25. Lux H. et al., 2016 Plasma Phys Control. Fusion **58**, 7, 075001
26. Lux H. et al., 2015 Fus. Eng. & Des. **101**, 42